



Wang, S., Li, M., Patil, A., Sun, S., Tian, L., Zhang, D., ... Mann, S. (2017). Design and construction of artificial photoresponsive protocells capable of converting day light to chemical energy. *Journal of Materials Chemistry A*, 5, 24612-24616. <https://doi.org/10.1039/C7TA08999F>

Peer reviewed version

Link to published version (if available):
[10.1039/C7TA08999F](https://doi.org/10.1039/C7TA08999F)

[Link to publication record in Explore Bristol Research](#)
PDF-document

This is the author accepted manuscript (AAM). The final published version (version of record) is available online via the Royal Society of Chemistry at <http://pubs.rsc.org/en/Content/ArticleLanding/2017/TA/C7TA08999F#!divAbstract>. Please refer to any applicable terms of use of the publisher.

University of Bristol - Explore Bristol Research

General rights

This document is made available in accordance with publisher policies. Please cite only the published version using the reference above. Full terms of use are available:
<http://www.bristol.ac.uk/pure/about/ebr-terms>

Design and construction of artificial photoresponsive protocells capable of converting day light to chemical energy

Shengjie Wang,^{*a} Mei Li,^{*b} Avinash J Patil,^b Shiyong Sun,^c Liangfei Tian,^b Dongxiu Zhang,^a Meiwen Cao,^a Stephen Mann^{*b}

[a] State Key Laboratory of Heavy Oil Processing and the Center for Bioengineering and Biotechnology, China University of Petroleum (East China), Qingdao, Shandong 266580 (China), E-mail: sjwang@upc.edu.cn

[b] Centre for Protolife Research and Centre for Organized Matter Chemistry, School of Chemistry, University of Bristol, Bristol BS8 1TS (UK), E-mail: mei.li@bristol.ac.uk or s.mann@bristol.ac.uk

[c] Department of Geological and Mineral Engineering, School of Environment and Resource, Southwest University of Science and Technology, Mianyang, Sichuan 621010 (China)

Abstract: We present a new strategy for the design and construction of artificial photoresponsive protocells based on the encapsulation and activation of metallized peptide/porphyrin self-assembled nanofilaments within silica nanoparticle-stabilized colloidosomes. The protocells exhibit high light sensitivity and can utilise day light (700 lux) for the production of nicotinamide adenine dinucleotide (NADH) by photo-mediated reduction of NAD⁺ within the colloidosomes. The results provide a promising step towards artificial photosynthetic micro-compartmentalized devices with integrated functional structures and photoresponsive behaviour.

Transformation of sunlight into chemical energy in photosynthesis is associated with an integrated photosystem comprising organized arrays of chlorophyll pigments and metal clusters to facilitate light capture, electron charge separation, and transfer and conversion into energy-storage molecules such as adenosine triphosphate (ATP) and reduced nicotinamide adenine dinucleotide phosphate (NAD(P)H). Mimicking the mechanisms of natural photosynthesis¹ using photosensitizers such as organic dyes,² metal complexes³ and hybrid graphitic carbons⁴ is receiving wide ranging attention for the development of novel materials capable of photo-electronic, photo-chemical and photo-catalytic transformations.⁵ Recently, Park and coauthors⁶ constructed an artificial photosynthesis complex in which the regeneration

of NADH was completed under visible light provided that an electron mediator was used to overcome the mis-matched energy levels between the light harvesting and catalytic units. In contrast, electron charge separation and transfer in photosynthesis are closely coupled by highly organized stacking and cooperation among different units⁷ to produce a highly efficient energy-transfer process involving long range exciton coherence.⁸ The prerequisite for a delocalized coupled excited state across the full length of the chlorophyll aggregate represents a major challenge for artificial photosynthesis as stacking disorders in synthetic porphyrin assemblies often restrict the exciton coherence to small domains that result in ineffective electron transmission.⁹

Herein, we report the preparation of a multi-functional photoactive assembly consisting of integrated structural, light harvesting and electron charge separation/transfer components based on the template-directed organization of tetrakis(4-sulfonatophenyl)porphine (TPPS) J-aggregates and catalytic platinum (Pt) nanoparticles on the surface of self-assembled peptide (Ac-IIIKK-NH₂ (I₄K₂); I = isoleucine, K = lysine) nanofilaments. Our objective is to initiate steps towards light-to-chemical conversion systems based on compartmentalization of integrated light harvesting and photoactive functionalities within dispersed synthetic cell-like structures (protocells) as a route to the design and construction of an “artificial alga” (Figure 1). To this end, we fabricated novel semi-permeable photoresponsive protocells via the encapsulation and activation of metallized peptide/porphyrin (I₄K₂/TPPS/Pt) fibrils within silica nanoparticle-stabilized colloidosomes capable of exhibiting a range of biomimetic and cell-like functions such as membrane gating,¹⁰ enzyme-induced small molecule signaling,¹¹ *in situ* gene expression,¹² enzyme-mediated catalysis,^{10,12,13} capsule growth and division,¹⁴ and enzyme-directed secretion of an extracellular-like matrix.¹⁵ Encapsulation of the photoactive I₄K₂/TPPS/Pt complex within the colloidosomes produced photoresponsive protocells that exhibited efficient coordination of light capture and electron transfer as demonstrated by the conversion and storage of day light (700 lux) into chemical energy in the form of NADH production within the colloidosomes.

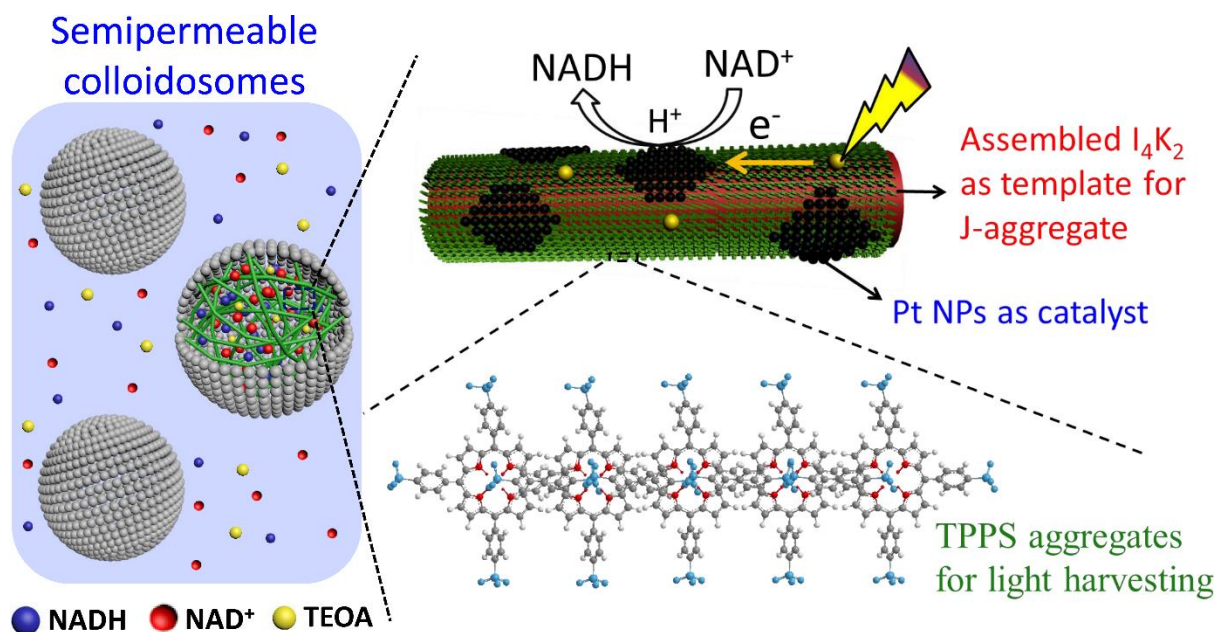


Figure 1. Schematic showing design and construction of artificial photoresponsive protocells. Photoactive colloidosomes were prepared from silica nanoparticle-stabilized water-in-oil Pickering emulsions containing an aqueous dispersion of I₄K₂/TPPS/Pt nanofilaments. The silica membrane was crosslinked with tetraethoxysilane and the colloidosomes transferred into water using established procedures¹⁰ to produce water-dispersible colloidosomes that were permeable to small molecules such as NAD⁺ and NADH (left panel). The I₄K₂/TPPS/Pt complex consisted of an integrated hierarchical organization of multi-functionalized twisted nanofilaments that were assembled in aqueous solution prior to encapsulation (right panel; see Methods). I₄K₂ peptide assemblies provide scaffolds/templates for TPPS deposition and mediate TPPS assemble into ordered J-aggregates in which photoexcited TPPS captures electrons from TEOA (the sacrificial electron donor) and transfers to Pt nanoparticles via TPPS aggregates. Pt nanoparticles increase the separation and transfer efficiency of electrons. Exposure of the I₄K₂/TPPS/Pt-containing colloidosomes to day light resulted in photo-mediated reduction of NAD⁺ specifically within the protocells and subsequent formation of NADH.

Hierarchically organized I₄K₂/TPPS/Pt nanofilaments were prepared prior to encapsulation via a three-step procedure involving molecular peptide self-assembly, electrostatic complexation and porphyrin assembly, and self-metallization (Figure 2A). Circular dichroism (CD) spectra of aqueous acidic solutions of I₄K₂ (pH 2.5) showed peaks at 197 and 219 nm that were characteristic of β -sheet formation (Figure S1). Corresponding TEM images indicated that the solutions contained self-assembled twisted nanofilaments of I₄K₂ that were uniform in width (typically 10 nm across) and a few micrometres in length (Figure 2B). These observations were consistent with lateral stacking and twisting of the primary β -sheet

nanostructures (Figure 2A) due to intermolecular hydrophobic and electrostatic interactions in association with molecular chirality.¹⁶ Addition of TPPS (50 μ M) to an aqueous dispersion (2 mM, pH 2.5) of pre-assembled I₄K₂ nanofilaments increased the extent of fibre bundling to produce thicker nanostructures with more roughened surfaces (Figure 2C). Energy-dispersive X-ray (EDX) analysis on the filaments detected sulphur (Figure S2), consistent with binding of TPPS anions at the positively charged surface of the I₄K₂ nanostructure. Significantly, peaks at 490 and 705 nm in the UV-vis spectra (Figure S3A), and a “split Cotton effect” at 489 nm in the CD spectra (Figure S3B) indicated that self-assembly of TPPS into a J-aggregate arrangement occurred in the presence of the I₄K₂ nanofibers at pH 2.5.¹⁷ This was consistent with fluorescence spectra of the I₄K₂/TPPS nanofilaments, which when compared with TPPS monomers in solution showed a weak emission at 600-750 nm (410 nm excitation) and quenched emission at 490 nm excitation, consistent with J-aggregate formation (Figure S4).¹⁸

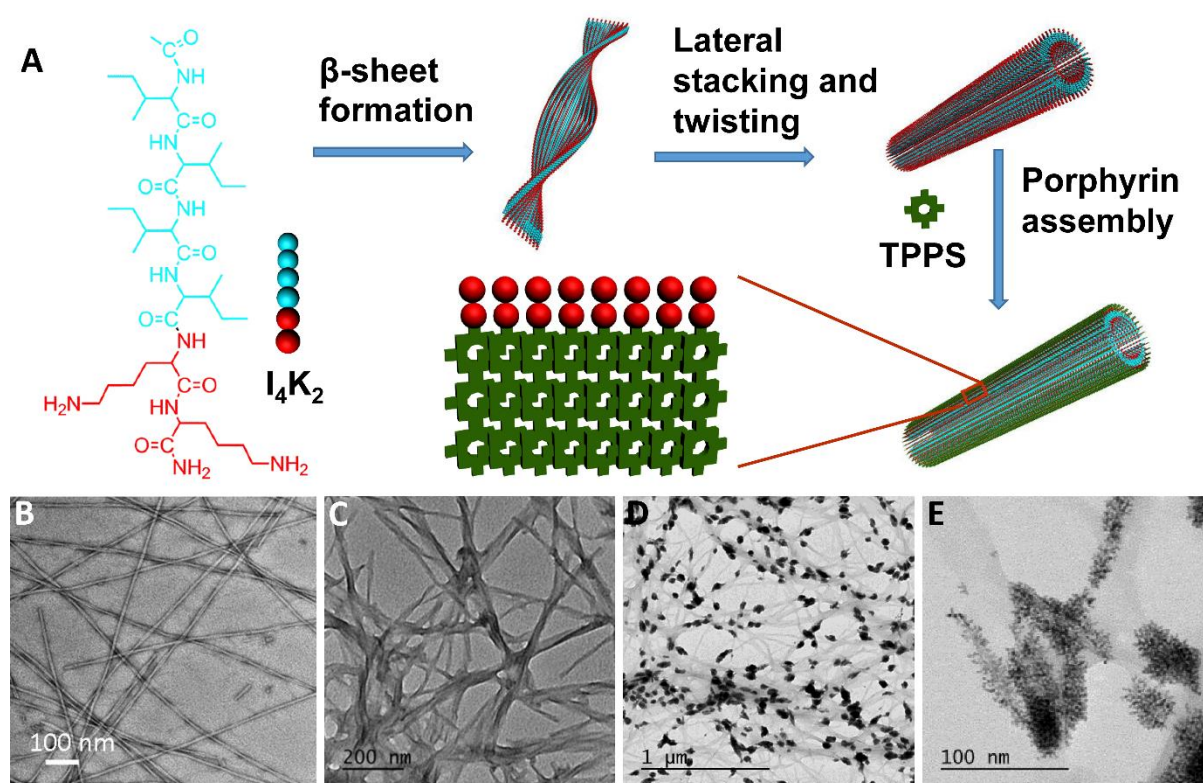


Figure 2. Formation of hierarchically organized I₄K₂/TPPS/Pt photoactive nanofilaments. (A) Molecular structure of I₄K₂ and proposed self-assembly into I₄K₂ and the I₄K₂/TPPS nanofilaments; the latter comprise a peptide core and porphyrin shell consisting of β -sheet and J-aggregate organized domains, respectively. TEM images showing nanofilaments of I₄K₂ (B), I₄K₂/TPPS (C), I₄K₂/TPPS/Pt (D,E). Formation of discrete Pt nanoparticles in

association with the surface of the I₄K₂/TPPS nanofilaments is observed at high magnification (E).

As no J-aggregates were detected at pH 2.5 in the absence of the I₄K₂ nanofilaments (Figure S3A), the results suggested that binding of the sulfonate negative charges of TPPS to cationic lysine groups on the surface of the I₄K₂ nanofilaments decreased the electrostatic repulsion between neighbouring TPPS anions, which in turn facilitated side-on J-state aggregation of the porphyrin molecules. As a consequence, the I₄K₂/TPPS nanofilaments consisted of a β -sheet structured peptide core surrounded by an organized shell of J-aggregate stacked porphyrin molecules. Given this integrated arrangement and the potential of the organized I₄K₂/TPPS nanofilaments to serve as a structured nanoscale platform for light harvesting, we extended the functionality towards light-induced electron charge separation and transfer by metallization of the nanofiber surface via photoreduction of an aqueous K₂PtCl₄/ascorbic acid solution for 30 min. As a result, Pt nanoparticles were specifically deposited on the surface of the I₄K₂/TPPS nanofilaments (Figure 2D), suggesting that the surface of the hybrid nanofibers acted as a preferential site for Pt reduction or nucleation, or both.¹⁹ TEM images showed intact nanofilaments associated with 30-80 nm clusters of 3 nm-sized electron dense particles (Figure 2E), which were confirmed as metallic Pt by lattice imaging and EDX analysis (Figure S5).

The photocurrent responses of the TPPS, I₄K₂/TPPS and I₄K₂/TPPS/Pt, nanofilaments were investigated by mounting the samples onto an indium tin oxide (ITO) coated glass anode immersed in 1M Na₂SO₄ solution containing 0.5% L-ascorbic acid as an electron donor. In all cases, the nanofilaments exhibited prompt, steady and reproducible photocurrent responses during repeated on/off cycles of visible light illumination (100 mW cm⁻²) (Figure 3). However, the photocurrent response for the I₄K₂/TPPS/Pt nanofilaments (7 μ A cm⁻²) was considerably enhanced compared with the non-metallated I₄K₂/TPPS sample ((2 μ A cm⁻²) and non-aggregated TPPS sample (less than 0.5 μ A cm⁻²) determined under similar experimental conditions. This enhancement was ascribed to the efficient charge separation and efficient electron transfer from the photoexcited TPPS moiety to the ITO glass specifically in the presence of the organized Pt nanoparticles.

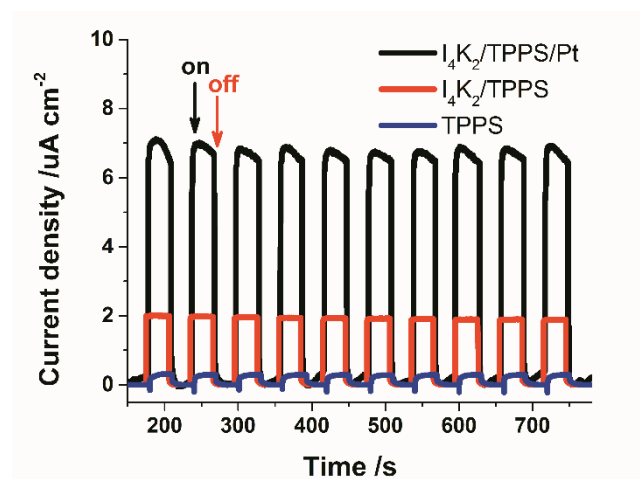


Figure 3. Photocurrent response of TPPS, $I_4K_2/TPPS$ and $I_4K_2/TPPS/Pt$ nanofilaments under visible light illumination in 1M $Na_2SO_4/0.5\%$ L-ascorbic acid solution with the applied potential at open circuit potential. Illumination from a 300 W xenon lamp (420 nm cut-off filter) was interrupted every 30 seconds.

The above results indicated that dispersions of $I_4K_2/TPPS/Pt$ nanofilaments could be prepared by a process of hierarchical self-assembly and functionalization and exhibited excellent photocurrent response behaviour. As a step towards a photoresponsive synthetic protocell we encapsulated the metallized peptide/porphyrin nanofilaments within silica nanoparticles (20-30 nm) (Figure S6) stabilized colloidosomes (Figure 1). Optical microscopy images of $I_4K_2/TPPS/Pt$ -containing colloidosomes recorded before and after transfer into water showed well-defined spherical hollow micro-compartments that were polydisperse and between 15 to 30 μm in diameter (Figure 4A,B). Fluorescence microscopy images showed red fluorescence or no fluorescence within the water-dispersed colloidosomes when excited at 385-410 (Figure 4C) or 450-490 nm (Figure S7), respectively, indicating that the J-aggregate porphyrin/peptide nanofilaments remained intact after encapsulation and were retained in the protocells after phase transfer.

The ability of the $I_4K_2/TPPS/Pt$ -containing colloidosomes to function as photoresponsive protocells capable of spatially localized light harvesting and chemical energy conversion was investigated by incubating the micro-compartments in an aqueous solution containing a membrane permeable electron acceptor (NAD^+ , 1 mM)

and electron donor (triethanolamine, TEOA, 15 w/v%). The reaction dispersions were exposed to either a 35000 lux light source or placed under day light (700 lux), and formation of NADH within the protocells monitored by increases in absorption at 340 nm (Figure S8).²⁰ Spectra recorded after 60 min of light exposure showed a strong 340 nm absorption band for samples placed under 35000 lux (Figure 4D). Onset of NADH production within the protocells was detected spectroscopically after 10 min of exposure at 35000 lux and increased at an approximately linear rate over a period of 1 h to a maximum NADH concentration of *ca.* 0.25 mM (Figure 4E). TEM studies showed that the initial organized structure of the I₄K₂/TPPS/Pt nanofilaments remained intact after 1 h of irradiation at 35000 lux, indicating that the complex was stable under illumination (Figure S9). Longer periods of light exposure at 35000 lux resulted in a decrease in NADH concentration due to partial oxidation of the photo-generated product as confirmed by control experiments on solutions of NADH exposed to the same light source (Figure S10). Moreover, control experiments based on the exposure of TPPS, I₄K₂/TPPS and I₄K₂/TPPS/Pt nanofilaments to a 35000 lux light source were shown in Figure 4F and Figure S11. The I₄K₂/TPPS/Pt nanofilaments exhibited highest conversion of NADH among them, that was consistent with the trends of the photocurrent response in Figure 3. This further indicated the function of Pt nanoparticle arrangements in accelerating the separation and transfer of photogenerated electrons.

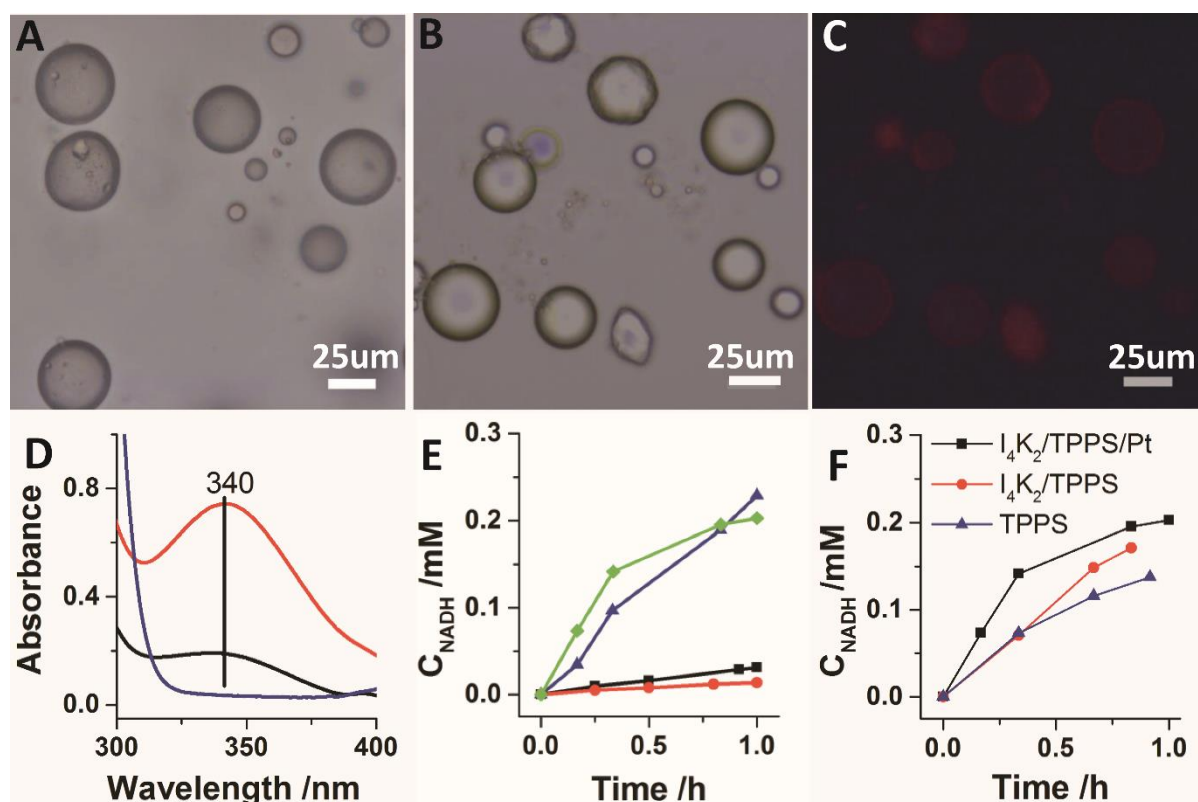


Figure 4. (A,B) Optical microscopy images of I_4K_2 /TPPS/Pt-containing cross-linked colloidosomes dispersed in oil as water-in-oil Pickering emulsions (A), and after transfer to water (B). (C) Fluorescence microscopy image of I_4K_2 /TPPS/Pt-containing colloidosomes recorded in water showing red fluorescence associated with TPPS J-aggregates. (D) UV-vis spectra recorded from suspensions of I_4K_2 /TPPS/Pt-containing colloidosomes after 1 h of exposure to 35000 lux light (red profile) or day light (700 lux, black profile). Peak at 340 nm corresponds to photo-mediated production of NADH within the protocells. No NADH formation is observed in the absence of NAD^+ (control, blue profile). (E) Plot showing increases in NADH concentration with time for I_4K_2 /TPPS/Pt-containing colloidosomes exposed to 35000 lux light (blue) or day light (700 lux, black). For comparison, free I_4K_2 /TPPS/Pt nanofibers exposed to 35000 lux light (green) and day light (red) are also shown. (F) Plot showing increases in NADH concentration with time for TPPS, I_4K_2 /TPPS and I_4K_2 /TPPS/Pt nanofilaments exposed to 35000 lux light.

Interestingly, exposure of the I_4K_2 /TPPS/Pt-containing colloidosomes under day light (700 lux) also showed generation of NADH albeit at a reduced rate (Figure 4D,E). Under these conditions and in contrast to exposure to the high intensity light source, photo-mediated conversion to NADH was dependent on the presence of Pt as well as integration of the metal catalytic nanoparticles, TPPS J-aggregates and I_4K_2 peptide nanofilaments (Figure S11, S12). Mechanistically, we attributed this to the integration

and spatial coupling of the light harvesting and electron transfer components along the surface of the I₄K₂/TPPS/Pt nanofilaments. Also, we compared the light transformation efficiency of I₄K₂/TPPS/Pt nanofilaments and I₄K₂/TPPS/Pt-containing colloidosomes with an equal amount of I₄K₂/TPPS/Pt. As shown in Figure 4E, the colloidosomes exhibited higher conversion of NADH under weak light irradiation (700 lux). This may be attributed to a relative higher local concentration of functional nanofilaments in the colloidosomes as they are too large to escape from the semipermeable membrane. These results indicated that relative higher light transformation efficiency can be obtained via the strategy of encapsulating the I₄K₂/TPPS/Pt nanofilaments into colloidosomes. As a consequence, the I₄K₂/TPPS/Pt-containing colloidosomes possessed higher levels of sensitivity under day light compared with their non-assembled counterparts, suggesting that light to chemical energy conversion can be achieved specifically within protocells operating under relatively low light conditions.

In summary, hierarchically organized I₄K₂/TPPS/Pt nanofilaments capable of integrated light harvesting and electron charge separation and transfer were encapsulated within silica nanoparticle-stabilized colloidosomes as a step towards novel artificial photoresponsive protocells. The protocells were able to convert light to chemical energy in the form of NADH even under day light conditions. Our studies offer a novel approach to the construction of photoresponsive micro-compartmentalized materials, and provide new opportunities in cell-free synthetic biology (artificial algae), photoactive micro-reactor design, and colloid-based energy capture and storage.

Experimental Section

A full description of the experimental methods is provided in the supporting information. Briefly, the artificial photoresponsive protocells were prepared via three steps: (a) assembly of J-aggregates of TPPS on the surface of preassembled I₄K₂ nanofilaments, (b) *in situ* photoreduction of Pt^{II} to produce a light responsive complex in the form of I₄K₂/TPPS/Pt nanofilaments, and (c) encapsulation of I₄K₂/TPPS/Pt nanofilaments within semi-permeable silica nanoparticle-stabilized colloidosomes to produce photoresponsive

protocells. Transformation of light to chemical energy within the protocells was demonstrated by generation of NADH from NAD⁺, and monitored by UV-vis spectroscopy.

Conflicts of interest: There are no conflicts of interest to declare

Acknowledgements

This work was supported by the EPSRC UK (EP/L002957/1), National Natural Science Foundation of China (21773310, 21473255, 41672039), Fundamental Research Funds for the Central Universities (15CX05017A) and Foundation of China Scholarship Council.

Keywords: artificial photoresponsive protocells • integrated functional nanostructures • hierarchical organization • biomimetic synthesis • photosynthesis

References

1. a) N. S. Lewis, G. Crabtree, *Basic Research Needs for Solar Energy Utilization*. Office of Science, U. S. Department of Energy: Washington, DC, **2005**, pp139-144; b) M. R. Wasielewski, *Acc. Chem. Res.* **2009**, *42*, 1910-1921.
2. a) K. T. Oppelt, E. Woss, M. Stiftinger, W. Schofberger, W. Buchberger, G. Knor, *Inorg. Chem.* **2013**, *52*, 11910-11922; b) D. H. Nam, C. B. Park, *ChemBioChem* **2012**, *13*, 1278-1282.
3. B. Xue, Y. Li, F. Yang, C. F. Zhang, M. Qin, Y. Cao, W. Wang, *Nanoscale* **2014**, *6*, 7832-7837.

4. a) J. H. Huang, M. Antonietti and J. Liu, *J. Mater. Chem. A* **2014**, *2*, 7686-7693; b) J.-J. Wang, J. Wang, K. Feng, H.-H. Zhang, Z.-J. Li, B. Liu, C.-H. Tung, L.-Z. Wu, *J. Mater. Chem. A* **2017**, *5*, 9537-9543.
5. a) A. Magnuson, M. Anderlund, O. Johansson, P. Lindblad, R. Lomoth, T. Polivka, S. Ott, K. Stensjo, S. Styring, V. Sundstrom and L. Hammarstrom, *Acc. Chem. Res.* **2009**, *42*, 1899-1909; b) T. Shikanai, *Curr. Opin. Biotechnol.* **2014**, *26*, 25-30; c) D. Q. Duanmu, C. Bachy, S. Sudek, C. H. Wong, V. Jimenez, N. C. Rockwell, S. S. Martin, C. Y. Ngan, E. N. Reistetter, M. J. van Baren, D. C. Price, C. L. Wei, A. Reyes-Prieto, J. C. Lagarias, A. Z. Worden, *Proc. Natl. Acad. Sci. U. S. A.* **2014**, *111*, 15827-15832; d) Y. Feng, W. F. Li, J. Li, J. W. Wang, J. P. Ge, D. Xu, Y. J. Liu, K. Q. Wu, Q. Y. Zeng, J. W. Wu, C. L. Tian, B. Zhou, Yang, M. J., *Nature* **2012**, *491*, 478-482; e) X.-B. Li, Y.-J. Gao, Y. Wang, F. Zhan, X.-Y. Zhang, Q.-Y. Kong, N.-J. Zhao, Q. Guo, H.-L. Wu, Z.-J. Li, Y. Tao, J.-P. Zhang, B. Chen, C.-H. Tung, L.-Z. Wu, *J. Am. Chem. Soc.* **2017**, *139*, 4789-4796.
6. J. H. Kim, M. Lee, J. S. Lee, C. B. Park, *Angew. Chem. Int. Ed.* **2012**, *51*, 517-520.
7. a) J. L. McHale, *J. Phys. Chem. Lett.* **2012**, *3*, 587-597; b) H. Imahori, T. Umeyama, K. Kurotobi, Y. Takano, *Chem. Commun.* **2012**, *48*, 4032-4045.
8. a) K. Hosomizu, M. Oodoi, T. Umeyama, Y. Matano, K. Yoshida, S. Isoda, M. Isosomppi, N. V. Tkachenko, H. Lemmetyinen, H. Imahori, *J. Phys. Chem. B* **2008**, *112*, 16517-16524. b) S. Okada, H. Segawa, *J. Am. Chem. Soc.* **2003**, *125*, 2792-2796.
9. A. Satake, Y. Kobuke, *Org. Biomol. Chem.* **2007**, *5*, 1679-1691.
10. M. Li, R. L. Harbron, J. V. M. Weaver, B. P. Binks, S. Mann, *Nat. Chem.* **2013**, *5*, 529-536.
11. S. Sun, M. Li, F. Dong, S. Wang, L. Tian, S. Mann, *Small* **2016**, *14*, 1920-1927.
12. M. Li, D. C. Green, J. L. R. Anderson, B. P. Binks, S. Mann, *Chem. Sci.* **2011**, *2*, 1739-1745
13. C. Wu, S. Bai, M. B. Ansorge-Schumacher, D. Wang, *Adv. Mater.* **2011**, *23*, 5694-5699.
14. M. Li, X. Huang, S. Mann, *Small* **2014**, *10*, 3291-3298
15. K. Akkarachaneeyakorn, M. Li, S. A. Davis, S. Mann, *Langmuir* **2016**, *32*, 2912-2919.

16. a) S. Wang, J. Xue, Y. Zhao, M. Du, L. Deng, H. Xu, J. R. Lu, *Soft Matter* **2014**, *10*, 7623-7629; b) S. Wang, J. Xue, X. Ge, H. Fan, H. Xu, J. R. Lu, *Chem. Commun.* **2012**, *48*, 9415-9417.
17. a) A. Romeo, M. A. Castriciano, R. Zagami, G. Pollicino, L. M. Scolaro, R. F. Pasternack, *Chem. Sci.* **2017**, *8*, 961-967; O. Arteaga, A. Canillas, Z. El-Hachemi, J. Crusats, J. M. Ribo, *Nanoscale* **2015**, *7*, 20435-20441; c) L. Zhang, M. Liu, *J. Phys. Chem. B* **2009**, *113*, 14015-14020.
18. a) V. V. Serra, N. G. B. Neto, S. M. Andrade, S. M. B. Costa, *Langmuir* **2017**, *33*, 7680-7691; b) J. V. Hollingsworth, A. J. Richard, M. G. H. Vicente, P. S. Russo, *Biomacromolecules* **2012**, *13*, 60-72.
19. K. Liu, R. Xing, C. Chen, G. Shen, L. Yan, Q. Zou, G. Ma, H. Möhwald, X. Yan, *Angew. Chem. Int. Ed.* **2015**, *127*, 510-515.
20. X. Huang, I. H. El-Sayed, X. Yi, M. A. El-Sayed, *J. Photochem. Photobiol. B: Biology* **2005**, *81*, 76-83.